ITC 4/52
Information Technology and Control
Vol. 52 / No. 4 / 2023
pp. 819-832
DOI 10.5755/j01.itc.52.4.33503

Melanoma Diagnosis Using Enhanced Faster Region Convolutional Neural Networks Optimized by Artificial Gorilla Troops Algorithm

Received 2023/02/27 | Accepted after revision 2023/08/09

HOW TO CITE: Nivedha, S., Shankar, S. (2023). Melanoma Diagnosis Using Enhanced Faster Region Convolutional Neural Networks Optimized by Artificial Gorilla Troops Algorithm. *Information Technology and Control*, 52(4), 819-832. https://doi.org/10.5755/j01.itc.52.4.33503

Melanoma Diagnosis Using Enhanced Faster Region Convolutional Neural Networks Optimized by Artificial Gorilla Troops Algorithm

S. Nivedha
Information and Communication Engineering, Anna University, Chennai, 600025, India

S. Shankar
Department of Computer Science and Engineering, Hindusthan College of Engineering and Technology, Coimbatore, 641050, India

Corresponding author: nivedhasubramanian@gmail.com

Melanoma, a rapidly spreading and perilous type of skin cancer, is the focus of this study, presenting a reliable technique for its detection. It is one of the most prevalent types of cancer that might be challenging for medical professionals to diagnose. Artificial intelligence can improve diagnostic accuracy when utilized in conjunction with the expertise of medical specialists. An innovative computer-aided method for the diagnosis of skin cancer has been introduced in the current study. The construction of the proposed method uses the African Gorilla Troops Optimizer (AGTO) Algorithm, a recently introduced meta-heuristic optimization algorithm, and deep learning models such as Faster Region Convolutional Neural Networks. To reduce the complexity of the analytic process, valuable features are chosen using the AGTO method, and further classification is implemented using Faster R-CNN. The proposed model is applied to the ISIC-2020 skin cancer dataset. When the final performance results from the proposed model are compared to those from four existing works, the findings show that the proposed system outperforms the existing models with an accuracy of 98.55%.

KEYWORDS: Deep learning, Skin Melanoma, Faster R-CNN, African Gorilla Troops Optimizer, Convolutional Neural Networks.

1. Introduction

Skin cancer has grown more quickly over the past ten years. Skin cancer comes in various forms, including Melanoma, Squamous cell carcinoma, Basal cell carcinoma, and Actinic keratosis. Investigations have proven that Melanoma can be more fatal than squamous cell carcinoma and actinic keratosis [2]. Just 9% of skin cancer cases are in the form of Melanoma, yet it causes 78% of fatalities. According to skin specialists, there is a 90% chance of identifying Melanoma if it is found in the initial phases [7]. It spreads to other body parts and becomes more challenging to treat if proper treatment is not administered in advance. In this instance, the diagnostic rate becomes even lower than 40%. Melanocytes and Ultraviolet emission are critical contributors to the development of skin cancer [9]. Skin cells develop quickly and become uncontrollable if the body's defense system cannot fix the damage. This first manifests as widening patches with blood loss, lumps, or sores that do not recover, which, if left untreated, can spread to other places [11].

Dermoscopy is used to determine skin cancer because it can be challenging to detect due to different skin characteristics or lesions. Dermoscopy examines the surface morphology of skin by using a multipolar magnifying lens and ambient illumination [12]. Compared to uncontrolled inspections, this method has a greater cancer detection rate. However, the detection accuracy solely depends on the therapist's competence. According to a recent survey, the therapist's accuracy in spotting skin cancer ranges from 78% to 86% [13].

Computer-based approaches or diagnostic methods based on computers are used to enhance classification precision. This process increases the use of computer vision techniques to analyze medical imagery for successful detection [10]. These methods aid in extracting additional pertinent aspects of the imagery, such as color schemes, patterns, irregularity, geometry, etc. Moreover, the characterization of the tumor depends on these parameters when employing technology-based methods. Capturing a skin tumor image, delineating tissue sections, character segmentation, etc., are crucial elements in machine-based diagnostic approaches. Skin lesions can be classified using several different techniques [18].

Several machine learning approaches are available in the healthcare industry [25], and they are effective from disease detection to assessment, regenerative medicine to fabrication, and investigation to medical studies [16]. In the realm of dermatology, the same tendency is being observed in the evaluation and supposition of malignant regions. The opportunity exists to move away from the traditional physical resection medical tests and towards computer-assisted diagnosis systems using extracted features from images of pathological changes and feature interpretation by machine learning techniques [27]. The inference reached by the experienced dermatologist for metastatic Melanoma is supported by utilizing machine learning algorithms.

Additionally, appropriate solutions have been discovered for this problem in recent years due to the advancement of technology, especially artificial intelligence. Image processing approaches are progressing as effective strategies in the interim [23]. Using computer vision to analyze trends like cancer from imagery automatically decreases human error and speeds up detection. Additionally, the value of medical image processing is demonstrated by how it assists doctors and physicists in assessing illnesses and preserving individuals from potentially fatal risks. One of the most used techniques for processing images is deep neural networks. Current proposals for significant advancements in the study of visual systems rely on novel types of neural networks. CNNs are a subset of deep neural networks frequently employed in machine learning for voice and imagery analysis. The use of meta-heuristics in many applications has significantly increased recently. Using them for global optimization is one of its essential applications [17]. Several types of meta-heuristic algorithms have been created in recent years. Thus, the proposed research intends to employ African Gorilla Troops Optimizer to select optimal dataset features. Further, Enhanced Faster Region Convolutional Neural Networks are applied to classify Skin Melanoma.

1.1. Contributions to the Work

The main contributions of this work are as follows.

1 To propose a novel version of Convolutional Neural Networks, Enhanced Faster Region CNN, to

effectively classify Skin Melanoma as benign or malignant.

2 To extract the optimal features from the ISIC-2020 skin cancer dataset using the latest meta-heuristic optimization algorithm, such as African Gorilla Troops Optimizer.

3 To demonstrate the performance supremacy of the proposed deep learning model and optimizer algorithm by comparing it against the state-of-the-art models for skin cancer diagnosis.

1.2. Research Motivation

Skin cancer, including Melanoma, has significantly increased its prevalence and severity over the past decade. This highlights the need for improved detection and diagnosis techniques to address this growing health concern. Among the various forms of skin cancer, Melanoma has been proven to be more fatal than squamous cell carcinoma and actinic keratosis. Failure to administer proper treatment early leads to reduced diagnostic rates (below 40%) and increased difficulty in treating the disease. Skin cancer can be challenging to detect due to various skin characteristics and lesions. Dermoscopy, which examines the surface morphology of the skin using magnifying lenses and ambient illumination, has a higher detection rate than unaided visual inspection. Computer-based approaches utilizing computer vision techniques can enhance classification accuracy in skin cancer detection. These methods extract relevant features from medical images, such as color schemes, patterns, irregularities, and geometries, aiding in the characterization and classification of skin tumors. Machine learning approaches, including dermatology, have gained prominence in the healthcare industry for disease detection, assessment, and medical studies. In dermatology, computer-assisted diagnosis systems based on machine learning algorithms can support dermatologists' evaluations and conclusions regarding malignant regions. With advancements in technology, especially artificial intelligence and image processing techniques, the potential for automated analysis of medical imagery, including cancer detection, has grown. Computer vision methods reduce human error and expedite the detection process. Deep neural networks, particularly convolutional neural networks (CNNs), are widely used for image-processing tasks, including skin cancer classification. Meta-heuristic algorithms offer the potential for selecting optimal dataset features for improved classification accuracy.

1.3. Paper Organization

The remainder of the paper is organized as follows. Section 2 briefs the literature on the existing machine learning and deep learning models for skin disease predictions. Section 3 discusses the proposed methodology for Melanoma diagnosis using Enhanced Faster R-CNN and African Gorilla Troops Optimizer; Section 4 elaborates on the results obtained on implementing the proposed algorithm for the ISIS-2020 dataset. Section 5 concludes the present research.

2. Related Works

Infection and bacteria are the causes of skin disorders. Many methods have been applied to the visuals to detect skin conditions in their beginning phases. The discovery of skin conditions in plants and people has been reviewed so that researchers can choose effective strategies based on their particular requirements [15]. Moreover, comparisons have been made between several approaches, including case-based inferences, intelligent agents, and color scheme visual recovery algorithms, on various characteristics, including precision, consistency, efficiency, size, and output coherence [30]. These methods illustrate the findings for a skin lesion using categorization methods. Moreover, choosing a predictor for cancer detection is a challenging issue because it affects the quality of the results. For a better understanding of various approaches, criteria, and strategies for selecting the classifier for the identification of cancer cells, a study was published in [10]. This section provides a summary of several notable research findings in this area.

A novel hybrid technique utilizing Convolutional Neural networks and Support Vector Machines was put forth in [5] to identify skin cancer. The outcomes of their approach for various imagery contrasted with other methods like genetic algorithms and artificial neural networks. According to their findings, the suggested effort boosted accuracy results by 4.36%. Deep Neural Network was used in [4] to identify human skin cancer. Categorization techniques involving two and eight ways were used in the experiment on var-

ious skin cancer imagery. With the help of 136,340 clinical samples, a neural network such as CNN was trained [27]. Their method proved effective at identifying cancer in imagery.

Legitimate Raman Spectroscopy was proposed to identify skin cancer [22]. Researchers employed 659 photographic instances, and their strategy led to excellent precision. This strategy draws heavily on multivariate quantitative evaluations that combine basic vector error correction models with cluster analysis [24]. For the categorization of lesions, they employed modified linear regression. A novel method for enhancing the convolutional neural networks (CNN) input utilizing the output of visual masks to raise the efficiency of the classifier was put forth in [20]. To develop the datasets, investigators also used the semantic segmentation principle. Their findings showed increased categorization precision.

By using a cutting-edge method that employs the "split and attack" strategy, researchers in [12] built the system to distinguish serious infections. The technique is used with deep CNN models to obtain an overall precision of 98.67%. The authors of [6] employ a different CNN-based strategy to find skin disease at the initial stage. To improve the recognition results by reducing the generated error, they used an advanced whale heuristic algorithm that was naturally inspired. The thickness and hue properties were frequently used in [8] for skin cancer detection techniques. Before undergoing a feature extraction step, the image pixels are converted directly between color spaces. By rebuilding the Inception pre-trained CNN architecture model on the PH2 dataset, a transfer learning idea is used to address the computational limitations [14]. A stochastic attribute identification step is integrated to obtain a prediction performance of 97.8% to avoid the "curse of multiplicity" issue [28].

Authors created a thick feature set in [26] to segment benign and cancerous skin lesions. This tensor combines several components, including slope location features, hue, and rotation distribution attributes [29]. The Support vector machine tags the resultant vector in the subsequent phase. The same pattern can be seen in [3, 1, 19, 21], where the slope and feature responsive curve model is used to pinpoint the lesion location. The authors improved the performance of the system by implementing a de-noising model in the pre-processing layer. Table 1 provides a comparison of the existing studies for skin cancer detection.

The examination above determined that there is still substantial scope for development in skin lesion image processing despite technological improvements and various research projects. Furthermore, quick identification and classification of skin lesions are necessary for providing prompt medical intervention. To accomplish this, the proposed work is inspired to employ Artificial Gorilla Troops Optimizer and Faster Region Convolutional Neural Networks to enhance the overall categorization of skin lesions compared to the segmentation and classification techniques performed by many researchers in this area.

Table 1

Comparison of Existing Approaches for Melanoma Diagnosis

Reference	Technique adopted	Inference	Drawbacks
[4]	Fuzzy C-Means Clustering	Seeker Optimization was implemented, which produced an accuracy of 90.56%	Supports 2D color space only
[22]	CNN with ABC feature Optimization	Skin cancer was detected with improved precision on specific boundaries	Different characteristics like hue, size, and shape were not considered for categorization purposes
[20]	Deep Neural Networks	The proposed approach produced an accuracy of 93% based on visual attributes using a Multilayer framework	Dependent only on images captured through dermoscopy
[8]	Artificial Neural Networks and K Nearest Neighbor	Classified based on homogeneous and globular patterns	Only the texture of features is considered, with less focus on geometry
[28]	Artificial Neural Networks and Support Vector Machine	Employed ABCDE rule for classification and produced an accuracy of 89.5%	Varied image textures were not considered

3. Proposed Methodology

The proposed system combines the metaheuristic optimization algorithm, African Gorilla Troops Optimizer, and the deep learning model, Faster R-CNN. The architecture of the suggested model is shown in Figure 1. The architecture consists of preprocessing the input skin cancer images using techniques such as Histogram Equalization, Image Denoising, and Image Fragmentation. After the preprocessing stage, it is passed on to the feature selection stage, where the African Gorilla Troops Optimizer algorithm is applied. Finally, the Melanoma classification is implemented using the selected features by employing the Faster R-CNN deep model.

Figure 1
Proposed Architecture

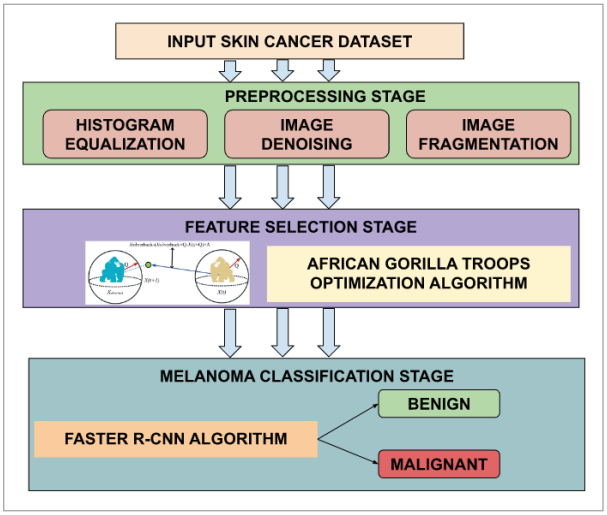

3.1. Preprocessing

The extraneous and bothersome portions of the input visuals are removed in this preliminary processing stage before moving on to the primary processing. In this stage, three preprocessing steps include histogram equalization, Image Denoising, and Image Fragmentation.

3.1.1. Histogram Equalization

There are many techniques used nowadays for improving images. Enhancing the intensity of the image is one option. The histogram equalization technique can boost the power of a poor-quality image so that the gray surface values are altered in the image to catch the entire spectrum. The fundamental concept is to map the varying illumination levels using a Cumulative Distribution Function as represented in (1).

$$X = F(a) = H - 1\int_0^i C_i(s)\,ds, \tag{1}$$

where F(a) is the transformation function to create the optimized histogram for the input image. After obtaining the histogram, it is essential to infuse uniformity in the histogram, which is defined as in (2),

$$X_b = F(a_b) = H - 1\sum_{c=0}^{b} C_i(i_c) = \frac{(H-1)}{(R-S)}\sum_{c=0}^{b} d_c, \tag{2}$$

where H denotes the optimal range of intensity in the image, R and S denotes the pixel count, i_c denotes the illumination level.

The standardized histogram and accumulated histogram of the input image must first be determined to produce an output image with a more balanced histogram. Then, the numbers must be converted to the range [0, H-1] by modeling each pixel in the input image with i_c illumination to a pixel corresponding to the luminance X_b.

3.1.2. Image Denoising

It is essential to utilize the proper noise removal techniques due to external noise in the images. Nonlinear polynomials are being used more frequently these days for picture synthesis. Dermoscopy imaging can occasionally contain noise due to the way they are generated. Thus, this issue must be fixed before moving on to the primary processing. Moreover, dermoscopy visuals may contain additional ambient noises that need removal. For this purpose, a weighted moving average method is adopted in this work. In this technique, a tiny window, known as a kernel, is slid across the entire imagery. Each pixel value of the image is altered with an average taken on the neighboring pixels of the particular pixel. This is represented as shown in (3),

$$S[x,y] = \frac{1}{(2a+1)^2}\sum_{i=0}^{N}\sum_{j=0}^{N} G[x+i, y+j]. \tag{3}$$

The above equation is applied when the weights are uniform in nature; in case of non-uniformity in conse-

quences, an additional function F needs to be added, as shown in (4),

$$S[x,y]=\sum_{i=0}^{N}\sum_{j=0}^{N}F[i,j]G[x+i,y+j]. \quad (4)$$

3.1.3. Image Fragmentation

Image leveling is a straightforward image fragmentation technique that separates the pixel value of an image into zero and one. Typically, the pixels are given a set-point value when leveling an embodiment. The pixels of the image are then compared to the set level; if the pixel illumination is higher than the set point, the pixel is converted to white; if smaller, the pixel is converted to black. As a result, a grayscale image or color image is transformed into a picture with a combination of black and white.

The median value for the input image utilizing the levels and the pixels is computed as shown in (5),

$$m_a = l(a)/K. \quad (5)$$

The set-point value for the image is determined using Equation (6),

$$SP(v)=T(0,r)+T(r,H), \quad (6)$$

where $T(0, r)$ is defined as given in (7) and $T(r, H)$ is defined as given in (8),

$$T(0,r)=\sum_{k=0}^{r-1}m_k \quad (7)$$

$$T(r,H)=\sum_{k=r}^{H-1}m_k. \quad (8)$$

The set point level is calculated using the sum of the median of all features in the input data. $T(0, r)$ represents the first half of the pixels, and $T(r, H)$ represents the second half. Both median is calculated and summed to find set point values. The results obtained after applying the preprocessing steps are shown in Figure 2.

Figure 2
Preprocessing Results

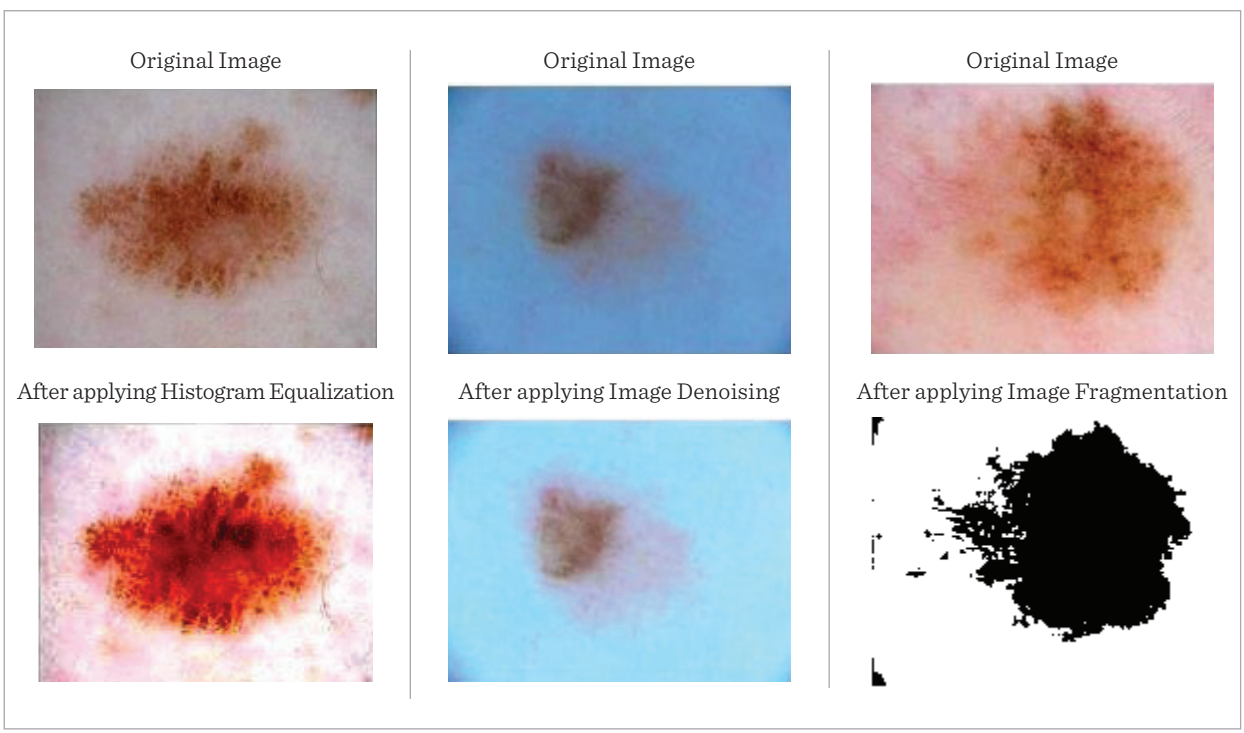

3.2. Artificial Gorilla Troops Optimizer

This section introduces a novel metaheuristic algorithm called Artificial Gorilla Troops Optimizer, which presents precise mathematical principles to describe the two phases of exploration and exploitation completely. The social behaviors of gorillas inspired this algorithm. This algorithm uses five distinct operators to simulate exploration and exploitation optimization methods focused on gorilla activities.

3.2.1. Phase of Exploration

Three different operations are carried out during the phase of exploration. Initially, it begins with a movement to the unknown spot, then to known places, and finally towards other gorillas. Considering three different conditions to represent these operations, a factor x is first chosen to decide the direction of a gorilla to an unknown spot. A move towards a strange place is assumed to occur whenever the element x is less than the rand. It is considered that if the rand is greater than or equal to 0.5, then there is a movement toward other gorillas in the group. Moreover, if the value of rand is less than 0.5, it can be inferred that there is a movement towards the known location. Equations (9)-(11) represent the conditions specified above for the three operations performed during the exploration phase,

$$F\left(k+1\right)=\left(Upper_b-Lower_b\right)\times s_1+Lower_b. \tag{9}$$

The above equations denote the movement to an unknown location, where s_1 is any value chosen randomly between 0 and 1. The mechanism of action towards the known spot is represented in (10),

$$F\left(k+1\right)=\left(s_2-D\right)\times A_s\left(k\right)+Y\times Z, \tag{10}$$

where D, Y and Z in the above equation are computed as shown in (11) to (13),

$$D=G\times\left(1-\frac{curr_{iter}}{tot_{iter}}\right) \tag{11}$$

$$G=\cos\left(2\times s_4\right)+1 \tag{12}$$

$$Y=D\times y, \tag{13}$$

where y is any value selected randomly between -1 to 1.

$$Z=P\times A\left(k\right). \tag{14}$$

The movement towards other gorillas in the group is denoted as shown in (15),

$$F\left(k+1\right)=A\left(j\right)-Y\times\left(Y\times\left(A\left(k\right)-\right.\right.\\ \left.\left.-FA_s\left(k\right)\right)\right)+s_3\times\left(A\left(k\right)-FA_s\left(k\right)\right). \tag{15}$$

At the end of this phase, the cost incurred for all the possible explorations is computed, and the optimum solution is considered the silverback.

3.2.2. Phase of Exploitation

This phase comprises two primary operations; in the first operation, all the young members of the gorilla group abide by the instructions given by the silverback chosen in the exploration phase. In the second operation, a quarrel occurs among the young gorillas once they grow up to determine the female gorillas.

The first operation to abide by the silverback is represented in (16),

$$F\left(k+1\right)=Y\times B\times\left(A\left(k\right)-A_{sb}\right)+A\left(k\right), \tag{16}$$

where $A\left(k\right)$ enotes gorilla location, represents the location of the gorilla chosen as the silverback.

$$B=(|\frac{1}{H}\sum_{j=1}^{H}FA_j\left(k\right)|^f)^{\frac{1}{f}} \tag{17}$$

$$f=2^Y. \tag{18}$$

The second operation of quarreling for adult females is represented in (19),

$$F\left(k\right)=A_{sb}-\left(A_{sb}\times T-A\left(k\right)\times T\right)\times M \tag{19}$$

$$T=2\times s_5-1 \tag{20}$$

$$M=\delta\times N. \tag{21}$$

The cost of all outcomes incurred from the operations in the exploitation phase is computed. As in the exploration phase, the most optimal solution is selected as the silverback. The algorithm for the African Gorilla troops optimizer is given in Figure 3.

Algorithm 1.

African Gorilla Troops Optimization Algorithm

Input: Population of Gorillas P and the total iterations required M

Output: Gorilla Position and survival rate

Step 1: Consider a group of the population $A_k\left(k=1,2,....,P\right)$

Step 2: Compute the Survival rate for Gorilla

Step 3: while (until end condition)

Step 4: Calculate D using (11)

Step 5: Calculate Y using (13)

Step 6: for each A_k

Step 7: Compute Gorilla movement using (9), (10) and (15)

Step 8: end for

Step 9: Compute Survival rate for Gorilla

Step 10: Compare FA with A, and make the replacement

Step 11: Update A_{sb} as the position of the chosen silverback

Step 12: for each A_k

Step 13: if (D>=1) then

Step 14: Compute Gorilla movement using (16)

Step 15: else

Step 16: Compute Gorilla movement using (19)

Step 17: end if

Step 18: end for

Step 19: Compute Survival rate for Gorilla

Step 20: Compare current outcomes with previous outcomes, and make the replacement

Step 21: Update A_{sb} as the position of the chosen silverback

Step 22: end while

Step 23: return $A_{optimalGorilla}$, $optialSurvivalrate$

3.2.3. Faster R-CNN

Faster Region Convolutional Neural Networks is a popular algorithm used for detecting objects in images and making classifications. There are generally three main components in a Faster R-CNN which serves for extracting features, identifying the regions and finally performing classification. Each of these components is composed of a neural network that enables rapid data computation.

Figure 3

Enhanced Faster R-CNN

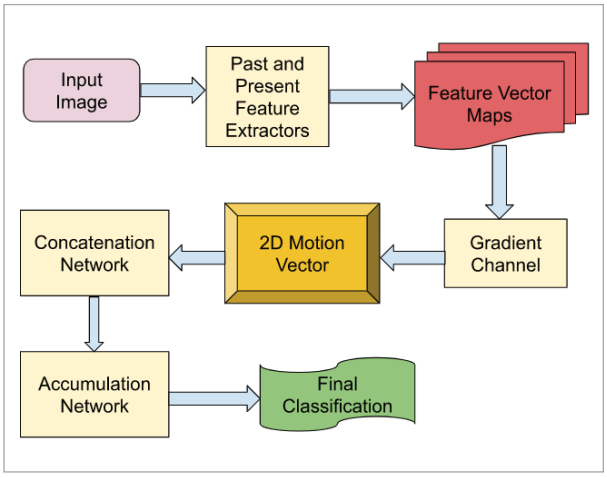

A densely interrelated CNN makes up this first component. This unit produces a set of selected features that characterize the parts of the image given an input image. A multivariate vector represents the feature map based on data around each image pixel. This component must be trained on many images to generate the feature maps. The second component is a convolutional neural network that extracts sections from an idea that contain the items from the feature set map produced by the first unit of the Faster R-CNN algorithm. Based on suggested regions and the quality set map, the third component, a fully connected neural network, predicts the category of an object and the exact position where it might be discovered.

3.2.4. Proposed Enhanced R-CNN

By combining the 2D features that were taken from the consecutive frames and adding them to the extra layers, 3D features were generated. A past Feature extractor, a present feature extractor, a gradient channel, a concatenation network, and an accumulation network comprise the five components of the proposed Enhanced Faster R-CNN framework, as shown in Figure 4.

The past and present Feature Extractors are employed to capture the attributes from the past and present sequences using the same methods as in the

first component of the conventional Faster R-CNN. Using a final CNN, the gradient channel identifies the 2D motion vector for each unit in the prior and present pixel. The motion vector of each pixel in the 2D direction is responsible for building the maps. Concatenation and accumulation networks are utilized to comprehend the attributes pattern generated from the preceding networks and obtain a 3D features matrix. There are two steps to functionalize. The concatenation network first enhances the primary features pattern, which adds a motion vector as independent vectors for each location. The accumulation network combines the present and past feature maps using a barrier design. The concatenation network involves collecting information from past attributes data and motion information that is crucial for Melanoma detection due to this processing. The accumulation network creates a features pattern that considers modifications in three levels and integrates it with the existing features pattern.

4 Results and Discussion

4.1. Dataset Description

The most complex Skin Melanoma dataset that is publicly accessible is the International Skin Imaging Collaboration (ISIC) dataset. One of the largest collections of high-resolution, quasi-skin images ever produced was manually classified into several tumor categories by a licensed physician. This dataset can create prediction models for actinic keratosis, basal and squamous cell carcinoma. However, we only choose data from the dataset specifically utilized for Melanoma detection to generate the model. Two thousand samples are used to train and evaluate the model above. Every image used for training, validation, and testing is an RGB image with various shapes, sizes, orientations, and ambient configurations. Moreover, several visuals have numerous distortions in them. The dataset used for the experimental purpose is available in the below link,

https://challenge.isic-archive.com/data/#2020

4.2. Experimental Setup

The experiments were implemented in the NVIDIA GPU on the Colab environment offered by Google. 25 GB of memory in the Titan RTX Tesla was utilized to execute the code in Python in the Keras framework. The backend environment for running the Python scripts was TensorFlow, which was carried out in a system with Ubuntu 21.04 as the operating system.

4.3. Performance Metrics

The metrics such as Accuracy, Sensitivity, Specificity and Precision are used to evaluate the performance of the proposed system. In the following metrics *TPOS*, *TNEG*, *FPOS*, *FNEG* denotes the true positive, true negative, false positive, false negative values.

$$Accuracy = \frac{TPOS + TNEG}{TPOS + TNEG + FPOS + FNEG} \tag{22}$$

$$Sensitivity = \frac{TPOS}{TPOS + FNEG} \tag{23}$$

$$Specificity = \frac{TNEG}{TNEG + FPOS} \tag{24}$$

$$Precision = \frac{TPOS}{TPOS + FPOS} \tag{25}$$

4.4. Experimental Results

The performance of the proposed model is evaluated on several criteria by varying the number of data samples, executing it on different epochs, by employing a 5-fold cross-validation technique. The results obtained on all the cases are discussed in this section. Table 2 contains the details of the metric values achieved for different numbers of training samples. Of the 2000 samples considered for training and validation purposes, 1500 samples are chosen for training and the remaining are reserved for testing. Initially, the proposed algorithm was run with 300 training samples, and the accuracy produced by the model was 97.66%. Further, the count of the training samples was gradually increased by 300 for four iterations 600, 900, 1200, and 1500. The accuracy was also increased progressively at 97.78%, 97.98%, 98.45%, and 98.98% for each increment of the training samples. Similarly, Sensitivity, Specificity, and Precision metrics are computed for every rise in the training data sample. The average values of Accuracy, Sensitivity, Specificity, and Precision are determined to be 98.16%, 96.47%, 98.29%, and 98.26%, respectively. Figure 5 compares the metric values generated for different training data samples.

Table 2
Performance Evaluation by varying the data samples

Data Samples	Accuracy (%)	Sensitivity (%)	Specificity (%)	Precision (%)
300	97.66	95.52	97.45	97.89
600	97.78	95.95	97.85	97.95
900	97.98	96.65	98.45	98.12
1200	98.45	96.78	98.75	98.56
1500	98.95	97.45	98.98	98.78
Average	98.16	96.47	98.29	98.26

Figure 5
Performance Evaluation by varying samples

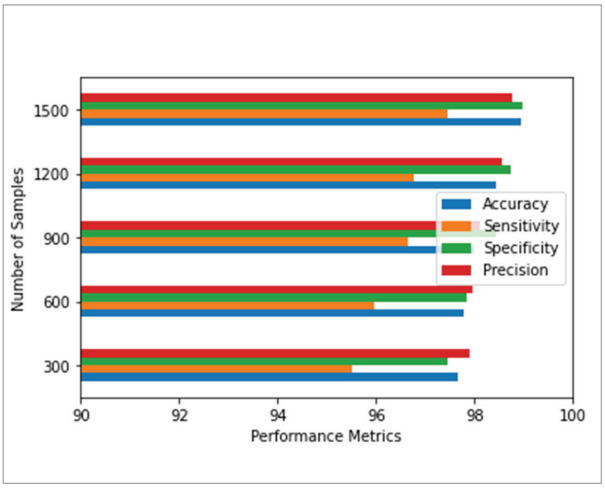

The 300 training samples were used initially, then gradually increased the sample size by 300 for four iterations until they reached 1500 samples. They evaluated the performance of the model based on different metrics, including accuracy, sensitivity, specificity, and precision, at each stage of training. The results show that the performance of the model improves as training samples increase. The accuracy increased gradually from 97.66% to 98.98%, while the sensitivity, specificity, and precision were also enhanced. The average values of these metrics across all stages of training were 98.16%, 96.47%, 98.29%, and 98.26%, respectively.

The performance results were also analyzed by differing the number of epochs for the deep learning model and provided in Table 3. The range of epochs considered for the experimental purposes are 50, 100, 200,

Table 3
Performance Evaluation by varying the number of epochs

Epochs	Accuracy (%)	Sensitivity (%)	Specificity (%)	Precision (%)
50	97.56	96.65	97.85	96.55
100	97.89	96.78	97.66	97.98
200	97.98	97.78	98.45	98.85
500	98.88	98.5	98.56	98.77
1000	98.98	98.66	98.88	98.89
Average	98.26	97.67	98.28	98.2

Table 4
Performance Evaluation by applying 5-Fold Cross Validation

Number of Folds	Accuracy (%)	Sensitivity (%)	Specificity (%)	Precision (%)
Fold 1	98.23	95.56	97.45	97.56
Fold 2	98.33	96.75	97.85	97.64
Fold 3	98.56	96.85	98.56	98.75
Fold 4	98.75	97.55	98.45	98.85
Fold 5	98.89	97.89	98.25	98.88
Average	98.55	96.92	98.11	98.34
Standard Deviation	0.2768	0.89739	0.4585	0.67419

500 and 1000. In aggregate, the model was run for 1000 epochs by cautiously increasing the number of epochs from 50 to 1000. The average Accuracy, Specificity, and Precision values were close at 98.26%, 98.28%, and 98.2%, respectively. The average weight of Sensitivity was achieved to be 97.67%. The accuracy value for varying epochs was almost standard, between 97% - 98%.

To avoid the overfitting problem in which the model fails to generalize to a particular pattern for prediction, fivefold cross-validation is employed in the proposed system. This technique mainly involves splitting the data into k folds and evaluating the capability of the model when given new data for making predictions. Table 4 contains the values obtained by applying 5-fold cross-validation to the ISIC 2020 dataset. The dataset is split into five folds in this evaluation to assess the model predictability. The accuracy values obtained for fold 1, fold 2, fold 3, fold four, and fold five validation are 98.23%, 98.33%, 98.56%, 98.75%, and 98.89%, respectively. The average accuracy value for all five folds is 98.55%. Similarly, the average sensitivity, specificity, and precision values are 96.92%, 98.11%, and 98.34%, respectively. The standard deviation values for all the metrics are also computed as well.

The performance of the proposed system is also contrasted against the existing works in the literature to demonstrate the performance supremacy of the proposed model. The existing works are carefully chosen, which employ a combination of deep learning models and meta-heuristic optimization algorithms for Skin Melanoma diagnosis. The current works considered include the work proposed in [12], which utilizes Support Vector Machine and Thermal Exchange Optimization, the model developed in [6], which incorporates Hybrid Deep Neural Network and Grasshopper Optimization algorithm, the research in [14], which involves Inception Convolutional Neural Networks along with Wildebeest Herd Optimizer and the work in [26] which uses Convolutional Neural Networks with African Vulture Optimizer for Skin disease prediction. The results generated are tabulated in Table 5. The accuracy of each model is 96.53% for SVM-TEO, 96.89% for HDNN-GHO, 97.56% for ICNN-WHO, and 97.89% for CNN-AVO. However, the accuracy produced by the proposed model is higher than the other existing models considered for comparison purposes, depicted in Figure 6. The proposed Faster R-CNN and African Gorilla Troops Optimizer produced an accuracy of 98.55%, a sensitivity of 96.92%, a specificity of 98.11%, and a precision of 98.34% is superior to the existing models taken for performance comparison.

The time complexity is analyzed in Table 5 by measuring the computation time of three algorithms Inception CNN, CNN, and Faster R-CNN in Python. The time CNN algorithms take is 32ms to predict the task where, whereas our proposed method takes only 18ms, less than existing models.

Table 5
Performance Comparison Existing Works Vs Proposed Work

Reference	Classification Technique	Optimization Algorithm	Accuracy (%)	Sensitivity (%)	Specificity (%)	Precision (%)	Time (ms)
[12]	SVM	Thermal Exchange Optimization	96.53	-	-	95.52	-
[6]	Hybrid DNN	Grasshopper Optimization	96.89	95.56	96.78	-	-
[14]	Inception CNN	Wildebeest Herd Optimizer	97.56	-	-	97.12	32ms
[26]	CNN	African Vulture Optimizer	97.89	96.53	97.25	97.56	32ms
-	Faster R-CNN	African Gorilla Troops Optimizer	98.55	96.92	98.11	98.34	18ms

Figure 6
Performance Comparison Existing Vs Proposed

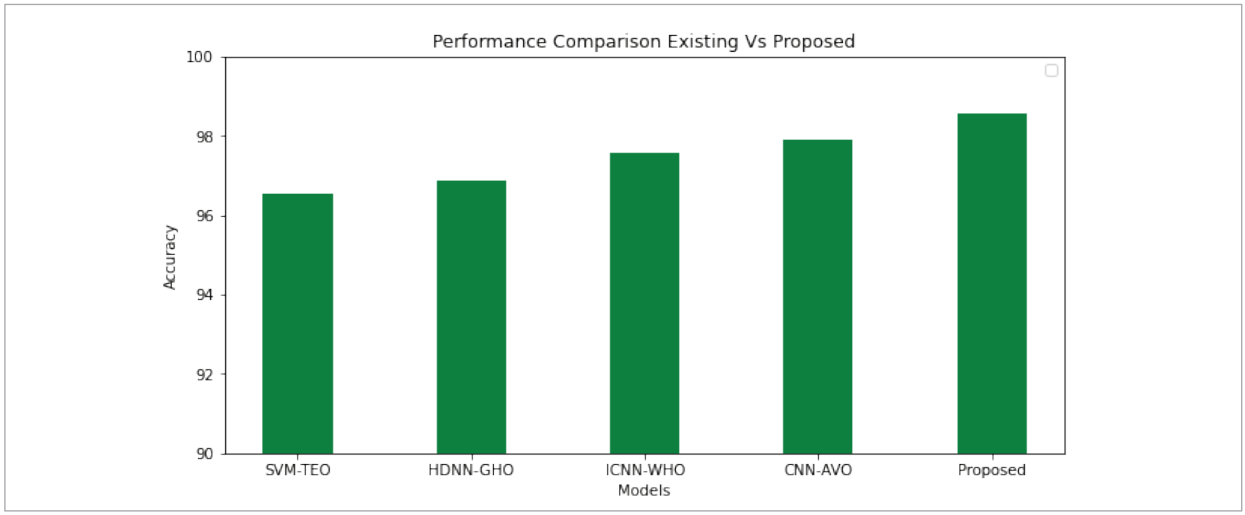

5. Conclusion

Malignant Melanoma represents the most menacing and hostile form of skin cancer. To tackle this issue, a promising avenue involves investigating computational intelligence approaches to classify skin ailments and identify skin tissue. The present study proposes a groundbreaking technique that employs deep learning and evolutionary algorithms to develop a highly efficient Melanoma diagnosis system. To alleviate the complexity of the approach, various main attributes are extracted from the image utilizing preprocessing techniques such as histogram equalization, image denoising, and image fragmentation. A recently established African Gorilla Troops Optimizer was suggested for feature selection, and the extracted features were then used to produce an ideal classification using Enhanced Faster R-CNN. The results showed that the proposed method performed best compared to the other existing works, with 98.55% accuracy for the ISIC-2020 dataset. Although the suggested plan is effective, its architecture combined deep learning and metaheuristics led to a complex configuration. As a result, future research work can focus on refining the proposed technique to develop a faster, less complicated, and more challenging method.

References

1. Abayomi-Alli, O. O., Damaševičius, R., Misra, S., Maskeliūnas, R., Abayomi-Alli, A. Malignant Skin Melanoma Detection using Image Augmentation by Oversampling in Nonlinear Lower-Dimensional Embedding Manifold. Turkish Journal of Electrical Engineering and Computer Sciences, 2021, 29, 2600-2614. https://doi.org/10.3906/elk-2101-133
2. Albahar, M. A., Skin Lesion Classification, Using Convolutional Neural Network with Novel Regularize. IEEE Access, 2019, 7, 38306-38313. https://doi.org/10.1109/ACCESS.2019.2906241
3. Almaraz-Damian, J.A., Ponomaryov, V., Sadovnychiy, S., Castillejos-Fernandez, H. Melanoma and Nevus Skin Lesion Classification using Handcraft and Deep Learning Feature Fusion via Mutual Information Measures. Entropy, 2020, 22(4), 484. https://doi.org/10.3390/e22040484
4. Amali, D., Dinakaran, M. Wildebeest Herd Optimization: A New Global Optimization Algorithm Inspired by Wildebeest Herding Behavior. Journal of Intelligent and Fuzzy Systems, 2019, 37(6), 8063-8076. https://doi.org/10.3233/JIFS-190495
5. Angurana, N., Rajan, A.P., Srivastava, I. Skin Cancer Detection and Classification. International Journal of Engineering and Management Research, 2019, 9. https://doi.org/10.31033/ijemr.9.2.13
6. Babino, G., Lallas, A., Agozzino, M., Alfano, R., Apalla, Z., Brancaccio, G. Melanoma Diagnosed on Digital Dermoscopy Monitoring: A Side-By-Side Image Comparison is needed to improve early Detection. J Am Acad Dermatol. 2021, 85(3), 619-25. https://doi.org/10.1016/j.jaad.2020.07.013
7. Bengani, S., Vadivel, S. Automatic Segmentation of Optic Disc in Retinal Fundus Images Using Semi-Supervised Deep Learning. Multimedia Tools and Applications, 2021, 80(3), 3443-3468. https://doi.org/10.1007/s11042-020-09778-6
8. Brinker, T. J., Hekler, A., Enk, A. H., Berking, C., Haferkamp, S., Hauschild, A. Deep Neural Networks are Superior to Dermatologists in Melanoma Image Classification. European Journal of Cancer, 2019, 119, 11-7. https://doi.org/10.1016/j.ejca.2019.05.023
9. Codella, N. C., Nguyen, Q. B., Pankanti, S., Gutman, D. A., Helba, B., Halpern, A. C., Smith, J. R. Deep Learning Ensembles for Melanoma Recognition in Dermoscopy Images. IBM Journal of Research and Development, 2017, 61(4/5), 5-1. https://doi.org/10.1147/JRD.2017.2708299
10. Dorj, U. O., Lee, K. K., Choi, J. Y., Lee, M. The Skin Cancer Classification using Deep Convolutional Neural Network. Multimedia Tools and Applications, 2018, 77(8), 9909- 9924. https://doi.org/10.1007/s11042-018-5714-1
11. Esteva, A., Kuprel, B., Novoa, R. A., Ko, J., Swetter, S. M., Blau, H. M., Thrun, S. Dermatologist-Level Classification of Skin Cancer with Deep Neural Networks. Nature, 2017, 542(7639), 115-118. https://doi.org/10.1038/nature21056
12. Hagerty, J. R., Stanley, R. J., Almubarak, H. A., Lama, N., Kasmi, R., Guo, P., Drugge, R. J., Rabinovitz, H. S., Oliviero, M., Stoecker, W. V. Deep Learning and Handcrafted Method Fusion: Higher Diagnostic Accuracy for Melanoma Dermoscopy Images. IEEE Journal of Biomedical and Health Informatics, 2019, 23(4), 1385-1391. https://doi.org/10.1109/JBHI.2019.2891049
13. Hameed, N., Shabut, A. M., Hossain, M. A. Multi-Class Skin Diseases Classification. In 12th IEEE International Conference on Software. Knowledge, Information Management & Applications (SKIMA), 2018.
14. Hosny, K. M., Kassem, M. A., Fouad, M. M. Classification of Skin Lesions into Seven Classes using Transfer Learning with AlexNet. Journal of Digital Imaging, 2020, 33(5), 1325-34. https://doi.org/10.1007/s10278-020-00371-9
15. Kadampur, M. A., Al, Riyaee, S. Skin Cancer Detection: Applying a Deep Learning based Model Driven Architecture in the Cloud for Classifying Dermal Cell Images. Informatics in Medicine Unlocked, 2020, 18, 00282. https://doi.org/10.1016/j.imu.2019.100282
16. Khan, M. A., Akram, T., Sharif, M., Javed, K., Rashid, M., Bukhari, S. A. C. An Integrated Framework of Skin Lesion Detection and Recognition through Saliency Method and Optimal Deep Neural Network Features Selection, Neural Computer Application, 2019, 1-20. https://doi.org/10.1007/s00521-019-04514-0
17. Kumar, M., Alshehri, M., Alghamdi, R., Sharma, P., Deep, V. A de-ANN Inspired Skin Cancer Detection Approach Using Fuzzy C-Means Clustering. Mobile Networks and Applications, 2020, 25, 1319-1329. https://doi.org/10.1007/s11036-020-01550-2
18. Li, Y., Shen, L. Skin Lesion Analysis Towards Melanoma Detection Using Deep Learning Network. Sensors, 2018, 18(2), 556. https://doi.org/10.3390/s18020556
19. Maqsood, S., Damaševičius, R. Multiclass Skin Lesion Localization, and Classification using Deep Learning

Based Features Fusion and Selection Framework for Smart Healthcare. Neural Networks, 2023, 160, 238-258. https://doi.org/10.1016/j.neunet.2023.01.022

20. Navid, F. R. S., Ghadimi, R. N. A Hybrid Neural Network-World Cup Optimization Algorithm for Melanoma Detection. Open Medicine, 2018, 13, 9-16. https://doi.org/10.1515/med-2018-0002
21. Nawaz, M., Nazir, T., Masood, M., Ali, F., Khan, M. A., Tariq, U. Damaševičius, R. Melanoma Segmentation: A Framework of Improved DenseNet77 and UNET Convolutional Neural Network. International Journal of Imaging Systems and Technology, 2022, 32(6), 2137-2153. https://doi.org/10.1002/ima.22750
22. Razmjooy, N., Sheykhahmad, F.R., Ghadimi, N. A Hybrid Neural Network-World Cup Optimization Algorithm for Melanoma Detection. Open Medicine, 2018, 13, 9-16. https://doi.org/10.1515/med-2018-0002
23. Shrivastava, V. K., Parvathi, K., Multiclass Skin Lesion Classification Using Image Augmentation Technique and Transfer Learning Models. International Journal of Intelligent Unmanned Systems, 2021.
24. Sugiarti, Y., Na'am, J., Indra, D., Santony, J. An Artificial Neural Network Approach for Detecting Skin Cancer. TEL-KOMNIKA Telecommunication Computing Electronics and Control, 2019, 17(2), 788-793. https://doi.org/10.12928/telkomnika.v17i2.9547
25. Tang, T. Y., Zhanga, L., Neohb, S. C., Limc, C. P. Intelligent Skin Cancer Detection using Enhanced Particle Swarm Optimization. Knowledge-Based Systems, 2018, 158, 118-135. https://doi.org/10.1016/j.knosys.2018.05.042
26. Vasconcelos, F. F. X., Medeiros, A. G., Peixoto, S. A., Reboucas Filho, P. P. Automatic Skin Lesions Segmentation Based on a New Morphological Approach via Geodesic Active Contour, Cognit. Syst. Res. 2019, 55, 44-59. https://doi.org/10.1016/j.cogsys.2018.12.008
27. Xu, Z., Sheykhahmad, F. R., Ghadimi, N., Razmjooy, N. Computer-Aided Diagnosis of Skin Cancer based on Soft Computing Techniques. Open Medicine, 2020, 15(1), 860-871. https://doi.org/10.1515/med-2020-0131
28. Young, A. T., Vora, N. B., Cortez, J., Tam, A., Yeniay, Y., Afifi, L., Yan, D., Nosrati, A., Wong, A., Johal, A., Wei, M. L. The Role of Technology in Melanoma Screening and Diagnosis. Pigment Cell & Melanoma Research, 2020, 1-13. https://doi.org/10.1111/pcmr.12907
29. Yuan, Y., Chao, M., Lo, Y. Automatic Skin Lesion Segmentation with Fully Convolutional-Deconvolutional Networks, 2017. arXiv preprint arXiv:1703.05165. https://doi.org/10.1109/TMI.2017.2695227
30. Zghal, N. S., Derbel, N. Melanoma Skin Cancer Detection based on Image Processing. Current Medical Imaging, 2020, 16(1), 50-58. https://doi.org/10.2174/1573405614666180911120546